

## Perturbations and chaos in quantum maps

Darío E. Bullo and Diego A. Wisniacki\*

*Departamento de Física “J. J. Giambiagi”, FCEN, Universidad de Buenos Aires, 1428 Buenos Aires, Argentina*

(Received 23 May 2012; published 15 August 2012)

The local density of states (LDOS) is a distribution that characterizes the effects of perturbations on quantum systems. Recently, a semiclassical theory was proposed for the LDOS of chaotic billiards and maps. This theory predicts that the LDOS is a Breit-Wigner distribution independent of the perturbation strength and also gives a semiclassical expression for the LDOS width. Here, we test the validity of such an approximation in quantum maps by varying the degree of chaoticity, the region in phase space where the perturbation is applied, and the intensity of the perturbation. We show that for highly chaotic maps or strong perturbations the semiclassical theory of the LDOS is accurate to describe the quantum distribution. Moreover, the width of the LDOS is also well represented for its semiclassical expression in the case of mixed classical dynamics.

DOI: [10.1103/PhysRevE.86.026206](https://doi.org/10.1103/PhysRevE.86.026206)

PACS number(s): 05.45.Mt, 05.45.Ac, 03.65.Sq

### I. INTRODUCTION

The response of quantum systems to external perturbations is a problem of paramount importance in many areas of physics. Many of the properties of complex quantum systems change dramatically when the system is perturbed, generating fundamental phenomena such as quantum phase transitions, irreversibility, or dissipation. The present development of experimental technics in complex quantum systems makes the understanding and characterization of the effects of perturbations highly desirable.

The most likely suitable means to characterize the effects of perturbations on quantum systems is the local density of states (LDOS). The LDOS, also called the strength function, was introduced by Wigner [1] to understand the statistical properties of the wave functions of complex quantum systems. The LDOS is the profile of an eigenstate of an unperturbed quantum system over the eigenbasis of its perturbed version. To be more specific, let us consider a system with a one-parameter-dependent Hamiltonian  $H(k)$  with eigenfrequencies  $\omega_j(k)$  and eigenstates  $|\psi_j(k)\rangle$ . The LDOS of an eigenstate  $|\psi_i(k_0)\rangle$  (that we call unperturbed) is given by

$$\rho_i(\omega, \delta k) = \sum_j |\langle \psi_j(k) | \psi_i(k_0) \rangle|^2 \delta(\omega - \omega_{ij}(k, k_0)), \quad (1)$$

with  $\omega_{ij}(k, k_0) = \omega_i(k_0) - \omega_j(k)$  and  $\delta k \equiv k - k_0$  the perturbation strength. Equation (1) shows that the LDOS is a density of states in which the  $\delta$  functions are weighed by the overlaps between perturbed and unperturbed states. In addition, the LDOS width gives an estimation of how many perturbed states contribute to an unperturbed one. Furthermore, it is the Fourier transform of the fidelity amplitude (FA) of the state  $|\psi_i(k_0)\rangle$ ,

$$\rho_i(\omega, \delta k) = \mathcal{F}[\langle \psi_i(k_0) | e^{iH(k)t/\hbar} e^{-iH(k_0)t/\hbar} | \psi_i(k_0) \rangle]. \quad (2)$$

Both the FA and its absolute square value, called the Loschmidt echo, are important measures of sensitivity to perturbations and irreversibility of quantum evolutions [2–6].

The LDOS has been considered in many contexts. In a seminal paper, Wigner studied the LDOS in a simple model of banded random matrices [1]. Subsequently, many authors have

used the LDOS to characterize the structure of the eigenstates of different random matrix models [7–9]. The LDOS has also been studied in several microscopic systems, for example, in a Ce atom [10], in chaotic billiards [11], or in a system of a particle that evolves in a smooth Hamiltonian [12]. In addition, the LDOS has been studied to characterize the effects of perturbations in the operation of quantum computers in the presence of static imperfections [13,14]. It was shown that, depending on the characteristics of the system, the LDOS has many regimes as a function of the perturbation strength  $\delta k$ . However, all the mentioned studies have revealed a region of perturbation strength in which the LDOS has a Lorentzian shape, which is usually called the Breit-Wigner distribution.

A step forward was recently made in the understanding of the LDOS for chaotic systems [15]. Its relation to the FA has been exploited to develop a semiclassical theory of the LDOS for locally perturbed billiards or maps, that is, when the perturbation is concentrated in a small region of the phase space accessible for the system. It was shown that the LDOS has a Lorentzian shape under very general perturbations of arbitrarily high intensity, and a semiclassical expression for its width was derived. This expression only depends on the perturbation, while the properties of the system are taken into account through a uniform measure in phase space. The same results were obtained in a subsequent publication for maps that are globally perturbed but the dynamics was assumed to be completely random [16].

The aim of our study is to test the validity of the semiclassical theory of Refs. [15,16] in quantum maps when the perturbation is applied in all the phase space and the dynamics of the classical map is not completely random. We also consider perturbations that act in any region of the phase space. We study the behavior of the LDOS for maps with different degrees of chaoticity and intensity of the perturbation. For this purpose we consider two of the most paradigmatic systems of quantum chaos studies: the perturbed cat map and the Harper map. We show that the semiclassical approximation of the width of the LDOS works very well even for systems with mixed dynamics in which chaos coexists with regular islands. The prediction of the Lorentzian shape of the LDOS is fulfilled for highly chaotic maps or when the intensity of the perturbation is big enough.

\*wisniacki@df.uba.ar

The paper is organized as follows. In Sec. II we introduce the dynamical systems that we have used for the numerical study, the cat and the Harper maps, and we describe the main characteristics of the classical and quantum dynamics of the maps. Section III is devoted to presenting the semiclassical theory of the LDOS [15,16]. The starting point of this theory is a semiclassical approximation of the fidelity amplitude called dephasing representation [17]. In Sec. IV we study the behavior of the LDOS for systems in several situations and test the validity of the semiclassical theory. We consider various degrees of chaoticity and intensities of the perturbation. We also compare the cases of local and global perturbations. Finally, we conclude with a summary of our results and some final remarks in Sec. V.

## II. SYSTEMS: MAPS ON A TORUS

A usual procedure to understand a complex behavior is to consider very simple systems in which such a phenomenon is observed. The most simple dynamical systems that develop all types of complexity are abstract maps. Owing to their simplicity, classical and quantum maps have been very important in the development of classical and quantum chaos [18–20]. Furthermore, many quantum maps have been implemented experimentally in previous studies [21–23].

In this paper we have used maps acting on a torus phase space of area  $\mathcal{A} = 1$ . In particular we have considered the well-known cat and Harper maps. These maps possess all the essential ingredients of chaotic and mixed dynamics and are extremely simple from a numerical point of view.

The cat maps are linear automorphisms of the torus that exhibit hard chaos. Anosov's theorem [24] establishes that the cat maps are structurally stable; that is, the orbits of a slightly perturbed map are conjugated to those of the unperturbed map by a homeomorphism. A perturbation of a cat map can be represented by matrices acting on the coordinates

$$\begin{bmatrix} q' \\ p' \end{bmatrix} = G \begin{bmatrix} q \\ p \end{bmatrix} + \begin{bmatrix} 0 \\ 1 \end{bmatrix} \epsilon(q, k) \pmod{1}, \quad (3)$$

where  $G$  is a  $2 \times 2$  matrix with integer elements chosen such that  $\text{Tr}(G) > 2$  and  $\det(G) = 1$  since the maps are hyperbolic and conservative. We consider a perturbation

$$\epsilon(q, k) = (k/2\pi)[\cos(2\pi q) - \cos(4\pi q)], \quad (4)$$

with the perturbation strength  $k < 0.11$  to satisfy the Anosov theorem [24,25]. To take into account different degrees of chaoticity, in this paper we have considered the following matrices  $G$ :

$$G_1 = \begin{pmatrix} 2 & 1 \\ 1 & 1 \end{pmatrix}, \quad G_2 = \begin{pmatrix} 80 & 6399 \\ 1 & 80 \end{pmatrix}.$$

The corresponding Lyapunov exponents, which determine the rate of exponential divergence of classical trajectories, are  $\lambda_1 \approx 0.96$  and  $\lambda_2 \approx 5.07$ . We note that  $\lambda$  is approximately uniform over the whole phase space and nearly independent of  $k$  [26].

Perturbed cat maps do not capture all the possible motions of Hamiltonian systems. The most common situation is a mixture of regular islands interspersed with chaotic regions. To consider this general situation the model that we have chosen

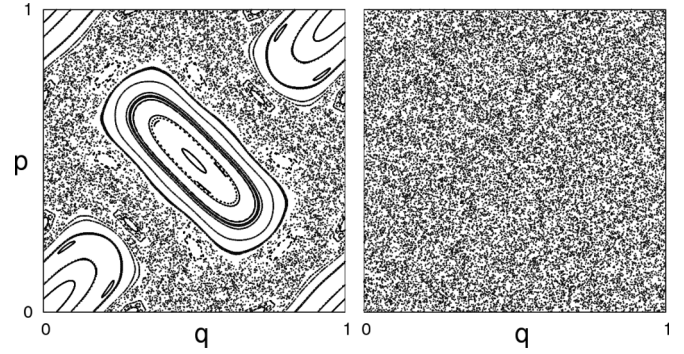


FIG. 1. Classical phase space of the Harper map for  $k = 0.3$  (left) and  $k = 200$  (right). See text for details.

to study is the Harper map in the unit square [27],

$$\begin{aligned} q' &= q - k \sin 2\pi p \pmod{1}, \\ p' &= p + k \sin 2\pi q' \pmod{1}, \end{aligned} \quad (5)$$

where  $k$  is a parameter that controls the behavior of the system. This map can be understood as the stroboscopic version of the flow corresponding to the (kicked) Hamiltonian

$$H(p, q, t) = \frac{1}{2\pi} \cos(2\pi p) + \frac{k}{2\pi} \cos(2\pi q) \sum_n \delta(t - nk). \quad (6)$$

This is an approximated Hamiltonian for the motion of an electron in a crystal under the action of an external field.

The Harper map presents a mixed dynamics that depends on the parameter  $k$ . Figure 1 shows some phase-space drawings for this model as an example of the underlying classical dynamics. As can be seen in Fig. 1 (left), the system presents a mixed dynamics with regions of regularity around the origin and the corners coexisting with chaos, in agreement with the Kolmogorov-Arnold-Moser theorem [24]. When the parameter  $k = 200$  the sizes of the islands are so small that it is not possible to observe them without a finer resolution [see Fig. 1 (right)].

The quantization on the torus implies that the wave function should be periodic in both position and momentum representations. If in the coordinate and momentum representations the wave function has a period 1 with spacing  $1/N$ , it follows that  $1 = 2\pi\hbar N$ . Then, we have a Hilbert space of  $N$  dimensions for a fixed value of  $\hbar$ . As  $N$  takes increasing values, we reach the semiclassical limit. The position basis  $\{q_i\}_{i=1}^{N-1}$  (with  $q_i = i/N$ ) and momentum basis  $\{p_i\}_{i=1}^{N-1}$  (with  $p_i = i/N$ ) are related by the discrete Fourier transform. In this setting a quantum map is simply a unitary  $U$  acting on an  $N$ -dimensional Hilbert space, and evolution after  $n$  steps is given by  $U^n$ .

There is no general method for map quantization. For the perturbed cat map we have considered the quantization based on the classical propagator of Refs. [18,25]. In this case, the matrix elements of the propagator in the position basis are

$$\begin{aligned} U_k^C(q', q) &= \sqrt{\frac{N}{ig_{12}}} \exp \left[ \frac{i\pi N}{g_{12}} (g_{11}q^2 - 2q'q + g_{22}q'^2) \right] \\ &\times \exp \left\{ \frac{ikN}{2\pi} \left[ \sin(2\pi q) - \frac{1}{2} \sin(4\pi q) \right] \right\}, \quad (7) \end{aligned}$$

where  $g_{i,j}$  are the elements of the matrix  $G$  and we have used  $g_{12} = 1$ .

For the Harper map [27], the matrix elements of the evolution operator in the mixed basis of position and momenta are

$$U_k^H(q, p) = e^{-iNk \cos(2\pi q)} e^{-iNk \cos(2\pi p)}. \quad (8)$$

### III. SEMICLASSICAL THEORY OF THE LDOS OF CHAOTIC MAPS

The LDOS as defined in Eq. (1) depends on the characteristics of the state  $|\psi_i(k_0)\rangle$ . To avoid any dependence on some particular characteristics of this state, an average over unperturbed states is performed. Owing to the finite number of states in quantum maps, we average over the entire Hilbert space. Thus, the averaged LDOS  $\rho(\omega, \delta k)$  is

$$\rho(\omega, \delta k) = \frac{1}{N} \sum_{i=1}^N \rho_i(\omega, \delta k). \quad (9)$$

The inverse Fourier transform of Eq. (9), the so-called average fidelity amplitude (AFA), is the starting point of the semiclassical approximation of the LDOS,

$$\overline{O(t, \delta k)} = \frac{1}{N} \sum_i \langle \psi_i(k_0) | e^{iH(k)t/\hbar} e^{-iH_0(k_0)t/\hbar} | \psi_i(k_0) \rangle. \quad (10)$$

To evaluate Eq. (10) we have used the so-called dephasing representation, a semiclassical formulation for fidelity amplitude which avoids the usual trajectory-search problem of the standard semiclassics [17]. One of the forms of the FA obtained using the dephasing representation is

$$O_\phi(t, \delta k) = \int W_\phi(q, p) e^{-i\Delta S_i(q, p, \delta k)/\hbar} dq dp, \quad (11)$$

where  $\Delta S_i(q, p, \delta k)$  is the action difference evaluated along the unperturbed orbit starting at  $(q, p)$  that evolves at a time  $t$ , and  $W_\phi(q, p)$  is the Wigner function of the initial state  $|\phi\rangle$ . Then,

$$\overline{O(t, \delta k)} = \int W(q, p) e^{-i\Delta S_i(q, p, \delta k)/\hbar} dq dp, \quad (12)$$

where  $W(q, p) = (1/N) \sum W_i(q, p)$ , with  $W_i(q, p)$  being the Wigner function of  $|\psi_i(k_0)\rangle$ . For chaotic systems, the mean value of the Wigner function for a base of eigenstates is approximately a uniform distribution so  $W(q, p) = 1/V$ , where  $V$  is the volume of the phase space. Therefore,

$$\overline{O(t, \delta k)} = \frac{1}{V} \int e^{-i\Delta S_i(q, p, \delta k)/\hbar} dq dp. \quad (13)$$

Time is discrete in maps, so from now on we use the integer  $n$  to count time steps and  $V$  is the area of the phase space that in our case is equal to unity.

In order to solve Eq. (13) for maps we need to assume that trajectories become uncorrelated between two successive hits in the perturbed region. This approximation is valid when the perturbation acts on an infinitesimal portion of the phase space [15, 28, 29] or if the unperturbed dynamics of the system is completely random [16].

Here we have considered the second case, the  $\lambda \rightarrow \infty$  limit, by assuming that the dynamics is purely random. This

evolution is completely stochastic in the sense that there is no correlation for the different times of the evolution. Then, to compute  $\overline{O(n, \delta k)}$ , we have divided the phase space into  $N_c$  cells. The probability to jump from one cell to any other in phase space is uniform. Therefore, it is straightforward to show that the mean FA results in

$$\begin{aligned} \overline{O(n, \delta k)} &= \sum_{j_1} \dots \sum_{j_n} e^{[-i(\Delta S_{j_1} + \dots + \Delta S_{j_n})/\hbar]} \\ &= \left( \sum_j e^{(-i\Delta S_j/\hbar)} \right)^n, \end{aligned} \quad (14)$$

where  $\Delta S_{jp}$  is the action difference evaluated in cell  $j$  at time  $p$ . The continuous limit is approached when  $N_c \rightarrow \infty$ , resulting in

$$\overline{O(n, \delta k)} = \left( \int e^{-i\Delta S(q, p, \delta k)/\hbar} dq dp \right)^n, \quad (15)$$

where  $\Delta S(q, p, \delta k)$  is the action difference after one step of the map.

The exponential decay of Eq. (15) can be rewritten as

$$\overline{O(n, \delta k)} = e^{-\Gamma n + i\varphi n}, \quad (16)$$

with

$$\Gamma = -\ln \left( \left| \int e^{-i\Delta S(q, p, \delta k)/\hbar} dq dp \right| \right). \quad (17)$$

and

$$\varphi = \arg \left( \int e^{-i\Delta S(q, p, \delta k)/\hbar} dq dp \right). \quad (18)$$

We note that  $\Gamma$  and  $\varphi$  depend on the perturbation strength  $\delta k$ .

Now, we obtain the semiclassical expression for the average LDOS by the inverse Fourier transform of Eq. (16),

$$\rho_{sc}(\omega, \delta k) = \mathcal{F}_{[\overline{O}]}^{-1}(\omega, \Gamma, \varphi) = \frac{\Gamma}{\pi[(\omega - \varphi)^2 + \Gamma^2]}. \quad (19)$$

The phase  $\varphi$  determines the location of the center of the Lorentzian function and  $\Gamma$  its width.

Finally, we have to take into account the fact that the spectrum of a map is periodic because of a compact phase space. This periodicity changes the form of the LDOS into a periodized Lorentzian function:

$$\begin{aligned} \rho_{sc}(\omega, \delta k) &= L^{(p)}(\omega, \Gamma, \varphi) \\ &= \sum_{j=-\infty}^{\infty} \frac{\Gamma}{\pi[(\omega - \varphi - 2\pi j)^2 + \Gamma^2]}. \end{aligned} \quad (20)$$

The same semiclassical expressions for the LDOS were obtained in Refs. [15, 28] when the perturbation acts in a region of the phase space of area  $\alpha \rightarrow 0$ .

A magnitude that has physical interest is the width  $\sigma$  of the LDOS, which is a measure of the number of perturbed states that are needed to describe an unperturbed one. Therefore, this quantity offers clear information about the effect of perturbations on a quantum system. Moreover, the width of the LDOS determines, for some regime of the perturbation, the rate of fidelity decay under imperfect motion reversal (the Loschmidt echo). There are different ways of determining this width of a distribution. In our case we take the distance

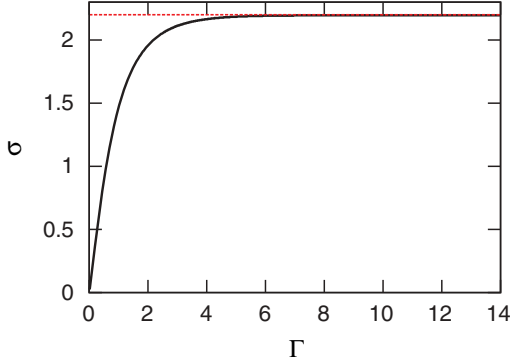


FIG. 2. (Color online) Width  $\sigma$  vs.  $\Gamma$  for a periodized Lorentzian function [Eq. (20)]. The limit of  $\sigma$  for  $\Gamma \rightarrow \infty$  which corresponds to a constant LDOS is plotted with a red dotted line.

about the average value of the LDOS that contains 70% of the probability. That is,

$$\int_{\langle\omega\rangle-\sigma}^{\langle\omega\rangle+\sigma} \rho(\omega, \delta k) d\omega = 0.7, \quad (21)$$

where

$$\langle\omega\rangle = \int_{-\pi}^{\pi} w \rho(\omega, \delta k) d\omega. \quad (22)$$

We show in Fig. 2 the relation between its width  $\sigma$  and  $\Gamma$  for the periodized Lorentzian function of Eq. (20).

#### IV. RESULTS

The main interest of a semiclassical theory is to describe quantum-mechanical quantities using classical information. In this section we show the behavior of the LDOS for the quantum maps presented before and test the validity of the semiclassical approximation of the LDOS described in the previous section. The aim in this section is to compare the approximated  $\rho_{sc}$  and  $\sigma_{sc}$  with the corresponding exact quantum values. The latter are numerically computed by diagonalization of the evolution operators of Eqs. (7) and (8).

The semiclassical approximation of the LDOS is completely determined by  $\Gamma$  and  $\varphi$  that are obtained with the calculation of the integral of Eq. (15). To avoid the dependence of the results with the dimension of the Hilbert space  $N$ , we have considered all the studied quantities as a function of the scaled strength of the perturbation,

$$\chi \equiv (k - k_0)/(2\pi\hbar) = \delta k N. \quad (23)$$

In all the calculations included in this section the number of states of the Hilbert space is set as  $N = 2000$ .

##### A. Perturbed cat map

The action difference for one iteration of the perturbed cat map described in Sec. II is given by

$$\Delta S(q, p, \delta k) = \left( \frac{\delta k}{4\pi^2} \right) \left[ \sin(2\pi q) - \frac{1}{2} \sin(4\pi q) \right]. \quad (24)$$

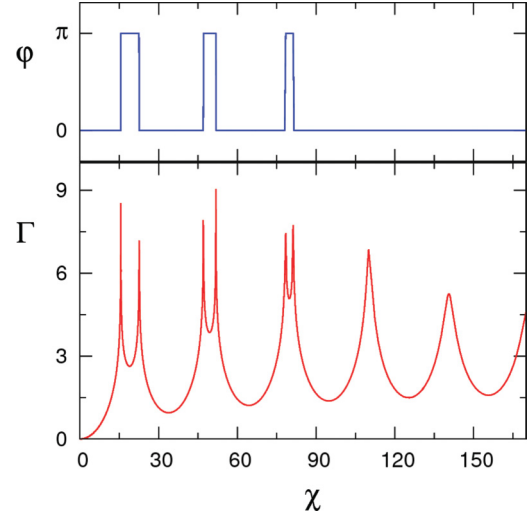


FIG. 3. (Color online)  $\Gamma$  and the phase  $\varphi$  as a function of the scaled perturbation  $\chi$  for the perturbed cat map.

Using Eqs. (24), (17), and (18) we compute  $\Gamma$  and  $\varphi$ . In Fig. 3 we plot  $\Gamma$  and  $\varphi$  for the perturbed cat map as a function of the scaled perturbation strength  $\chi$ . We can see that for perturbation of Eq. (4),  $\varphi$  has only two possible values either 0 or  $\pi$ .

We first compare the semiclassical approximation of the width of the LDOS with the corresponding quantum value. For this reason the width of the LDOS has been computed for the cat map using  $k_0 = 0.01$  to avoid all the arithmetic peculiarities of the cat map ( $k = 0$ ), which account for the nongeneric spectral statistics [30]. In Fig. 4 the width of the LDOS is shown for the cat maps with  $G_1$  and  $G_2$ . The semiclassical approximation  $\sigma_{sc}$ , plotted as a solid line, works extremely well for both cat maps in the whole range of considered perturbations.

The width of the LDOS  $\sigma$  for the cat maps has two clearly different regimes (Fig. 4). For small perturbation strength when  $\chi \lesssim 10$  it presents a quadratic behavior that is usually called the Fermi golden rule (FGR) regime. Conversely for greater strength the width is an oscillating function. In order to understand the behavior of  $\sigma_{sc}$  when  $\chi \rightarrow \infty$  we have used the

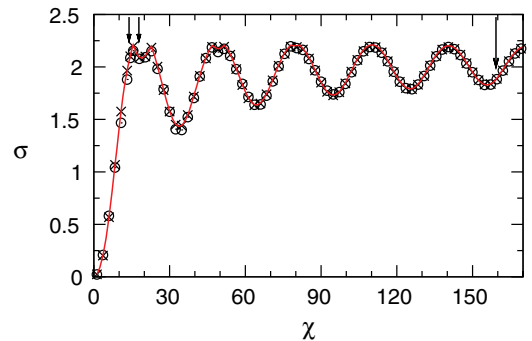


FIG. 4. (Color online) Width  $\sigma$  of the LDOS as a function of the scaled perturbation strength  $\chi = (k - k_0)N$  for the cat map with  $G_1$  ( $\circ$ ) and  $G_2$  ( $\times$ ). The red solid line is the semiclassical approximation of  $\sigma$ . The number of states of the Hilbert space is  $N = 2000$  and  $k_0 = 0.01$ . We indicate with arrows the perturbation strength of the LDOS displayed in Fig. 5.



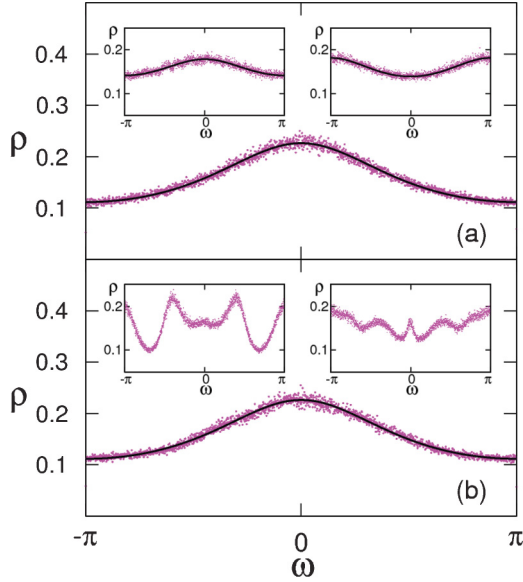


FIG. 5. (Color online) LDOS  $\rho$  (points) and its semiclassical approximation (solid line). (a) Cat map of Eq. (3) with  $G = G_2$  for a scaled perturbation strength  $\chi = 159.6$  (main plot),  $\chi = 14.4$  (left inset), and  $\chi = 18.0$  (right inset). (b) Cat map of Eq. (3) with  $G = G_1$  for  $\chi = 159.6$ ,  $\chi = 14.4$  (left inset), and  $\chi = 18.0$  (right inset).

stationary phase approximation method to solve the integral Eq. (13), obtaining

$$\Gamma \rightarrow -\ln[1/\sqrt{\chi}] \quad \text{for } \chi \rightarrow \infty;$$

therefore, the width  $\sigma_{sc} \rightarrow 0.7\pi$ , which corresponds to a uniform distribution.

At this point we would like to see how well the semiclassical approximation of the LDOS can describe the complete distribution. We have therefore computed the quantum LDOS for several values of perturbation strength for the cat maps  $G_1$  and  $G_2$ . In Fig. 5 we compare the LDOS with its semiclassical approximation for perturbations indicated in Fig. 4 with arrows. Figure 5(a) corresponds to the most chaotic case,  $G_2$ . In the main plot,  $\chi = 159.6$ ; in the left inset,  $\chi = 14.4$ ; and in the right inset,  $\chi = 18$ . We can see that the semiclassical approximation works very well for all the perturbations; that is, the LDOS is a periodized Lorentzian function independent of the perturbation strength. Left and right insets correspond to approximately the same width of the distribution but in the left figure  $\varphi = 0$  and  $\varphi = \pi$  for the right, so in this case the periodized Lorentzian is centered in  $\omega = \pi$ . As can be seen in Fig. 3, near  $\chi \approx 15$ , the phase  $\varphi$  has a discontinuity and jumps from 0 to  $\pi$ ; for this reason the center of the LDOS changes from  $\omega = 0$  to  $\omega = \pi$ . Similar behavior occurs in the other discontinuities of  $\varphi$  near  $\chi \approx 50$  and  $70$ .

In Fig. 5(b) the results for the cat map with the matrix  $G_1$  are shown. In the main figure panel, we show that for big perturbation strength after the quadratic regime ( $\chi = 159.6$ ) the LDOS is well described by the semiclassical Lorentzian distribution. Conversely for smaller perturbation strength the LDOS does not show Lorentzian behavior [see inset of Fig. 5(b)]. To understand this behavior we show

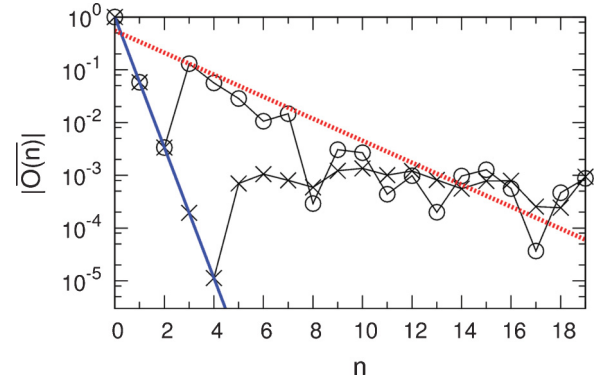


FIG. 6. (Color online) Mean value of the amplitude fidelity  $\overline{O(n)}$  for the cat map with  $G_1$  ( $\circ$ ) and  $G_2$  ( $\times$ ) with perturbation strength  $\chi = 14.4$ . The exponential decay given by  $\exp(-\Gamma n)$  is plotted with a solid blue line. We also plot with a dotted red line the exponential decay given by  $\exp(-\lambda n/2)$ , with  $\lambda$  the Lyapunov exponent for the cat map with  $G_1$ .

in Fig. 6 the mean value of the fidelity amplitude  $\overline{O(n)}$  for  $\chi = 14.4$  of both cat maps with  $G_1$  ( $\circ$ ) and  $G_2$  ( $\times$ ), which corresponds to the inverse Fourier transform of the LDOS plotted in the left inset of Figs. 5(a) and 5(b). We see that in the case in which the LDOS is not a periodized Lorentzian function the corresponding  $\overline{O(n)}$  has a big revival (at  $n = 4$ ). This kind of behavior, known as survival collapse, after which the largest revivals appear, was observed in a spin chain [31] and can be the cause for non-Markovian quantum evolutions [32].

We test now the validity of the semiclassical approximation of the LDOS for local perturbation. For this reason the perturbation is applied in a  $q$  strip from  $q_0 = 0.25$  to  $q_1 = 0.46$  so the area of the perturbed region is  $\alpha = \Delta q \Delta p = q_1 - q_0 = 0.21$ . In Fig. 7 we show  $\Gamma$  and  $\varphi$  as a function of the scaled perturbation strength  $\xi$  computed using Eqs. (17) and (18). We can see that for this local perturbation  $\varphi$  is an oscillating

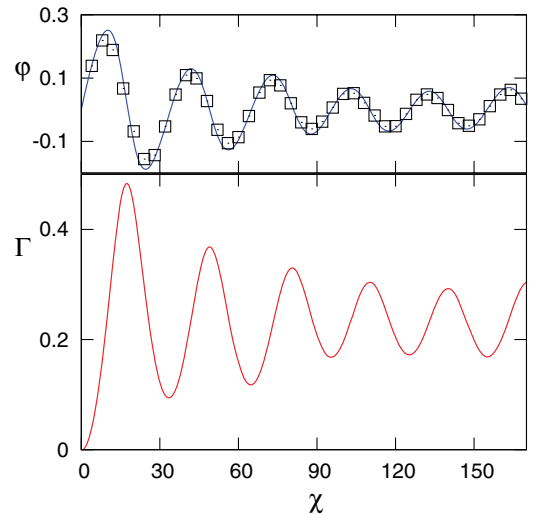


FIG. 7. (Color online)  $\Gamma$  and the phase  $\varphi$  as a function of the scaled perturbation  $\chi$  for the cat map when the perturbation is applied in a  $q$  strip from  $q_0 = 0.25$  to  $q_1 = 0.46$ . The mean value of the quantum LDOS is also plotted ( $\square$ ).

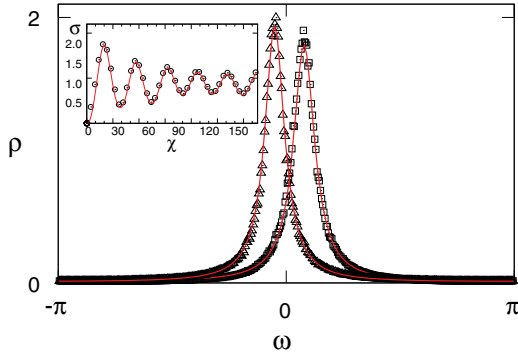


FIG. 8. (Color online) LDOS  $\rho$  for local perturbations. The cat map with  $G_1$  is perturbed from  $q_0 = 0.25$  to  $q_1 = 0.46$ . The scaled perturbation strength is  $\chi = 8$  ( $\Delta$ ) and  $\chi = 28$  ( $\square$ ). The semiclassical approximation of the LDOS is plotted with a red solid line. Inset: Width  $\sigma$  of the LDOS as a function of the scaled perturbation strength  $\chi$  ( $\circ$ ) and, plotted with a red solid line, the semiclassical approximation.

function so the semiclassical approximation of the LDOS is a periodized Lorentzian function with an oscillating mean value. In Fig. 7 (top) the mean value of the exact LDOS is also plotted ( $\square$ ), showing that the semiclassical  $\varphi$  describe very well this quantity.

The LDOS is also very well approximated by the semiclassical LDOS for all the perturbation strengths that we have studied. In Fig. 8 we show the LDOS for  $\chi = 8$  when the width grows quadratically (FGR regime) and for  $\chi = 28$  when the width shows an oscillating behavior. The semiclassical approximation is plotted with a solid line. In the inset of Fig. 8 we show the width of the LDOS for this local perturbation and its semiclassical approximation. We can clearly see that the  $\sigma_{sc}$  works very well for local perturbations. It is noteworthy that all the calculations for local perturbations were done using the map  $G_1$  showing that when the perturbation is applied in a small region of the phase space, a lesser degree of chaoticity is needed for the semiclassical LDOS to be accurate.

### B. Harper map

We have studied the LDOS of the Harper map using the evolution operator of Eq. (8) with  $k = k_0 + \delta k$ . The parameter  $\delta k$  is the perturbation strength and, as we used for the cat map, the scaled perturbation strength is  $\chi = \delta k N$ . In this case the action difference for one iteration of the Harper map is given by

$$\Delta S(q, p, \delta k) = \left( \frac{\delta k}{2\pi} \right) [\cos(2\pi p) + \cos(2\pi q')], \quad (25)$$

where  $q'$  is given by Eq. (5).

We have considered as an unperturbed system the cases with  $k_0 = 0.30$  [mixed dynamics, Fig. 1 (left)] and  $k_0 = 200$  [chaotic dynamics, Fig. 1 (right)]. Using Eqs. (17), (18), and (20), we compute  $\Gamma$ ,  $\varphi$ , and the corresponding semiclassical approximation of the LDOS. In Fig. 9 we show  $\Gamma$  as a function of the scaled perturbation strength  $\chi$ . For the action difference of the Harper map [Eq. (25)] we have obtained  $\varphi = 0$ .

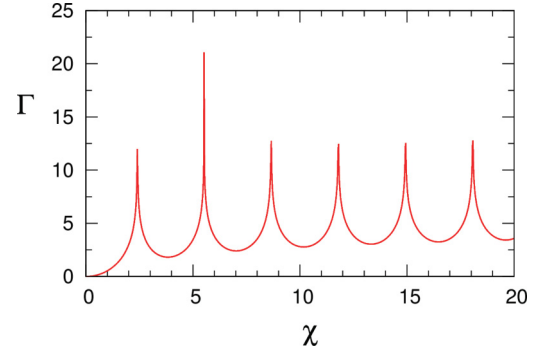


FIG. 9. (Color online)  $\Gamma$  as a function of the scaled perturbation strength  $\chi$  for the Harper map.

In Fig. 10 we show the width of the LDOS for the Harper map and the corresponding semiclassical approximation. When the dynamics of the Harper map is completely chaotic, the semiclassical  $\sigma_{sc}$  works well as expected. Surprisingly, the semiclassical approximation works reasonably well even for mixed dynamics. This agreement is more noticeable for bigger  $\chi$ . The explanation of this unexpected behavior is as follows. Equation (15) is exact for one time step ( $n = 1$ ), and if the perturbation strength is big enough the fidelity amplitude decays in this short time. Therefore, this short time decay gives the width of the Fourier transform, which is the LDOS.

In Fig. 11 we show the LDOS for the Harper map. Although the semiclassical width of the LDOS  $\sigma_{sc}$  works well for mixed dynamics, the complete distribution is not well reproduced by a periodized Lorentzian distribution. This is shown in the inset of Fig. 11(b) for the Harper map with  $k_0 = 0.3$  and  $\chi = 1.7$ . If the perturbation strength is bigger [Fig. 11 (a), main plot] the semiclassical theory works reasonably well but the quantum LDOS is a more fluctuating function than the chaotic case [see Fig. 11(a)]. As expected, the semiclassical theory works well for the case of  $k_0 = 200$  in which the Harper map is fully chaotic [Fig. 11(a)].

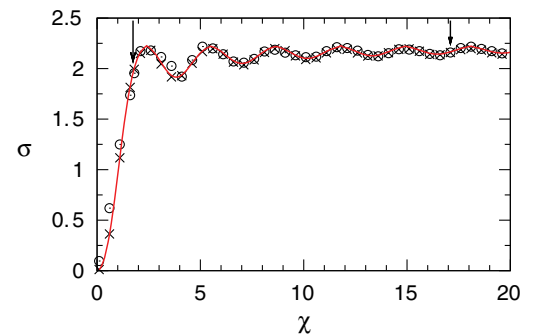


FIG. 10. (Color online) Width  $\sigma$  of the LDOS as a function of the scaled perturbation strength  $\chi$  for the Harper map with  $k_0 = 0.3$  ( $\circ$ ) and  $k_0 = 200$  ( $\times$ ). The semiclassical approximation  $\sigma_{sc}$  is plotted with a red line. We indicate with arrows the perturbation strengths of the LDOS displayed in Fig. 11.

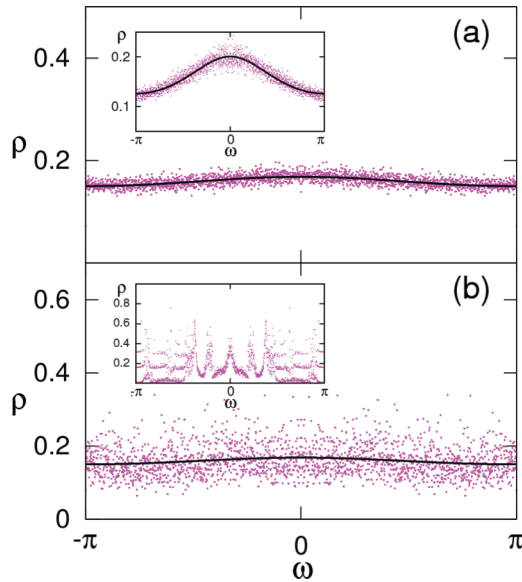


FIG. 11. (Color online)  $\rho$  (points) and its semiclassical approximation  $\rho_{sc}$  (solid line) for the Harper map. (a)  $k_0 = 200$ . In the main plot  $\chi = 17$  and in the inset  $\chi = 1.8$ . In both plots it is seen that the semiclassical LDOS describes the full quantum result. (b)  $k_0 = 0.3$  (mixed dynamics). In the main plot  $\chi = 17$  and in the inset  $\chi = 1.8$ .

### V. CONCLUSIONS

The reaction of a system to perturbations is a fundamental problem in quantum mechanics. In this paper we have made a detailed analysis of the response to perturbations of the simplest quantum systems, which can have complex classical dynamics. For this reason, we have studied the LDOS in the perturbed cat map, a completely chaotic system, and the Harper map, which has mixed dynamics. Our fundamental goal was to discuss the validity of a semiclassical theory of LDOS that was recently developed [15,16]. This theory is based on the relation of the LDOS with the fidelity amplitude, a measure of irreversibility and sensitivity to perturbations of quantum systems. Furthermore, it uses the dephasing representation of the fidelity amplitude, a semiclassical formulation that

avoids the usual problems of semiclassical theories. The main assumption of the semiclassical theory of LDOS is that the trajectories get uncorrelated after one step of the map. This condition is fulfilled if the dynamics is completely random or when the perturbation is applied in an infinitesimal region of the phase space. Owing to the fact that these conditions are not achieved in dynamical system, we tested the validity of such a semiclassical theory of the LDOS.

We have analyzed various situations involving local and global perturbations and also we have varied the degree of chaoticity. We show that the LDOS is very well described by its semiclassical expression when the map is highly chaotic, either if the perturbation is localized in phase space or when the perturbation strength is big enough. We remark that in these cases the semiclassical LDOS completely reproduces the quantum version without any fitting parameters. We have studied the case of mixed dynamics and surprisingly enough our results show that the semiclassical width of the LDOS describes the full quantum version even in this case.

We would like to highlight that our results could be of importance in the study of the LDOS of billiards. Indeed, the behavior of a billiard system has many resemblances to maps. For example, the classical dynamics of a billiard can be described by a map on the boundary. Quantum billiards are realistic systems that can be constructed in several experimental setups. In fact, there are cavities of microwaves, and acoustic or optical waves. The semiclassical approximation of the width of the LDOS has been successfully applied in a billiard that has been perturbed both locally [29,33] and globally [15]. However, in these works the behavior of the whole distribution was not properly discussed. Further insight on the LDOS of this systems will be part of future studies.

### ACKNOWLEDGMENTS

The authors acknowledge the support from CONICET (Grant No. PIP-6137), UBACyT (Grants No. X237, No. 20020100100741, and No. 20020100100483), and ANPCyT (Grant No. 1556). We would like to thank Ignacio García Mata for useful discussions.

[1] E. P. Wigner, *Ann. Math.* **62**, 548 (1955); **65**, 203 (1957).  
 [2] R. A. Jalabert and H. M. Pastawski, *Phys. Rev. Lett.* **86**, 2490 (2001).  
 [3] T. Gorin, T. Prosen, T. H. Seligman, and M. Žnidarič, *Phys. Rep.* **435**, 33 (2006).  
 [4] Ph. Jacquod and C. Petitjean, *Adv. Phys.* **58**, 67 (2009).  
 [5] D. A. Wisniacki and D. Cohen, *Phys. Rev. E* **66**, 046209 (2002).  
 [6] A. Goussev, R. A. Jalabert, H. M. Pastawski, and D. A. Wisniacki, *Scholarpedia* **7**, 11687 (2012).  
 [7] Y. V. Fyodorov, O. A. Chubykalo, F. M. Izrailev, and G. Casati, *Phys. Rev. Lett.* **76**, 1603 (1996).  
 [8] G. Casati, B. V. Chirikov, I. Guarneri, and M. Izrailev, *Phys. Lett. A* **223**, 433 (1996).  
 [9] Ph. Jacquod and D. L. Shepelyansky, *Phys. Rev. Lett.* **75**, 3501 (1995).  
 [10] V. V. Flambaum, A. A. Gribakina, G. F. Gribakin, and M. G. Kozlov, *Phys. Rev. A* **50**, 267 (1994).  
 [11] D. Cohen and E. J. Heller, *Phys. Rev. Lett.* **84**, 2841 (2000).  
 [12] D. Cohen and T. Kottos, *Phys. Rev. E* **63**, 036203 (2001).  
 [13] B. Georgeot and D. L. Shepelyansky, *Phys. Rev. E* **62**, 6366 (2000).  
 [14] G. Benenti, Giulio Casati, Simone Montangero, and Dima L. Shepelyansky, *Eur. Phys. J. D* **20**, 293 (2002).  
 [15] D. A. Wisniacki, N. Ares, and E. G. Vergini, *Phys. Rev. Lett.* **104**, 254101 (2010).  
 [16] I. García-Mata, R. O. Vallejos, and D. A. Wisniacki, *New J. Phys.* **13**, 103040 (2011).  
 [17] J. Vaníček, *Phys. Rev. E* **70**, 055201(R) (2004); **73**, 046204 (2006).  
 [18] J. H. Hannay and M. V. Berry, *Physica D* **1**, 267 (1980).

- [19] N. Balazs and A. Voros, *Europhys. Lett.* **4**, 1089 (1987).
- [20] J. P. Keating, *Nonlinearity* **4**, 309 (1991).
- [21] F. L. Moore, J. C. Robinson, C. F. Bharucha, B. Sundaram, and M. G. Raizen, *Phys. Rev. Lett.* **75**, 4598 (1995).
- [22] Y. S. Weinstein, S. Lloyd, J. Emerson, and D. G. Cory, *Phys. Rev. Lett.* **89**, 157902 (2002).
- [23] J. Chabé, G. Lemarié, B. Grémaud, D. Delande, P. Szriftgiser, and J. C. Garreau, *Phys. Rev. Lett.* **101**, 255702 (2008).
- [24] V. I. Arnold, *Geometrical Methods in the Theory of Ordinary Differential Equations* (Springer-Verlag, New York, 1988).
- [25] M. B. de Matos and A. M. Ozorio de Almeida, *Ann. Phys.* **237**, 46 (1995).
- [26] N. Ares and D. A. Wisniacki, *Phys. Rev. E* **80**, 046216 (2009).
- [27] P. Leboeuf, J. Kurchan, M. Feingold, and D. P. Arovas, *Phys. Rev. Lett.* **65**, 3076 (1990).
- [28] I. García-Mata and D. A. Wisniacki, *J. Phys. A: Math. Theor.* **44**, 315101 (2011).
- [29] A. Goussev, D. Waltner, K. Richter, and R. A. Jalabert, *New J. Phys.* **10**, 093010 (2008).
- [30] J. P. Keating and F. Mezzadri, *Nonlinearity* **13**, 747 (2000).
- [31] E. R. Fiori and H. Pastawski, *Chem. Phys. Lett.* **420**, 35 (2006).
- [32] I. García-Mata, C. Pineda, and D. A. Wisniacki, [arXiv:1204.3614](https://arxiv.org/abs/1204.3614).
- [33] B. Köber, U. Kuhl, H. J. Stöckmann, A. Goussev, and K. Richter, *Phys. Rev. E* **83**, 016214 (2011).